



THEORETICAL SIMULATION OF STRESS-STRAIN RELATIONS FOR SOME IRAQI CLAYS USING THE ENDOCHRONIC MODEL

Dr. Mohammed Yousif Fattah
Lecturer, University of Technology,
Building and Construction
Engineering Dept.

Maysm Th. Al-Hadidy
Assistant Lecturer, University of
Baghdad, College of Engineering,
Civil Engineering Dept.

Akeel A.S. Al-Gharbawi
Researcher, Ministry of
Reconstruction and Housing.

ABSTRACT

A constitutive law can be defined as a mathematical functional relation between physical quantities such as stress and strain and may take other factors like time ,temperature and additional material properties into account.

In this paper , the endochronic model is used to predict the stress-strain relations of two Iraqi clays. This model is a viscoplastic one but without introducing a yield surface. It encompasses material behaviour such that the current stress state is a function of strain history through a time scale called “intrinsic time” which is not the absolute time but a material property.

The simulation showed that the model overestimates the strains for all cases studied. This may be attributed to the material parameters which require a parametric study to determine their actual values for Iraqi clays.

KEYWORDS: Clay, Endochronic Model, Stress, Strain, Model Parameters

التمثيل النظري لعلاقات الإجهاد - الانفعال لبعض الأطيان العراقية باستعمال نموذج الزمن الضمني

الخلاصة

يمكن تعريف قوانين العلاقات التكوينية بأنها دوال رياضية تربط بين كميات فيزيائية مثل الإجهاد و الانفعال و قد تأخذ عوامل عديدة أخرى مثل الزمن و الحرارة و خصائص أخرى للمادة بنظر الاعتبار .
أستعمل في هذا البحث نموذج الزمن الضمني للنتبؤ بعلاقات الإجهاد-الانفعال لترتتين طينيتين عراقيتين . إن هذا النموذج هو من النوع اللدن - اللزج و لكنه لا يود خل سطح خضوع. و يعبر عن سلوك المادة بحيث أن حالة الإجهاد الحالية تكون دالة لتاريخ الانفعال من خلال مقياس زمني يدعى "الزمن الضمني" الذي يختلف عن الزمن المطلق من حيث أنه خاصية من خواص المادة. لقد بين التمثيل أن هذا النموذج يعطي قيمة عالية للانفعال لكل الحالات التي تمت دراستها. و يعزى هذا إلى معاملات المادة التي يتضمنها النموذج و التي تحتاج إلى دراسة معاملات لتحديد قيمها الحقيقية بالنسبة للترب الطينية العراقية.

INTRODUCTION

Endochronic theory was first introduced by Valanis in 1971. He coined this Greek name “Endochronic” that consists of two roots, endos (meaning inner) and chronos (meaning time). This

theory encompasses material behaviour such that the current stress state is a function of the strain history through a time scale called “intrinsic time” which is not the absolute time measured by a clock as in viscoplasticity but a material property. Hence, the endochronic theory is a “viscoplastic” one but without introducing a yield surface. Therefore, all the complexities and difficulties that develop in introducing a suitable yield criteria are avoided, (Valanis,1971).

Bazant in 1974 and later with his coworkers extended Valanis theory to predict the behaviour of different engineering materials such as concrete , and soils.

GENERALIZED CONSTITUTIVE RELATIONS:

To generalize the uniaxial concept of the endochronic theory into three dimensions, first, the definition of the intrinsic time increment, dz , which is used in stead of real time increment, dt , is introduced. The intrinsic time for time-dependent behaviour is function of strain increments, $d\epsilon_{ij}$ and time, dt . The dependence of dz upon $d\epsilon_{ij}$ is assumed to be gradual to exclude ideal plastic reponse. The function of dz will be continuous, smooth, and monotonically increasing. Thus, function $(dz)^s$ with an appropriate exponent ”s” , can be expanded in a tensorial power series in $d\epsilon_{ij}$ and dt , i.e., (Bazant and Bhat,1976):

$$(dz)^s = p + p_{ij} d\epsilon_{ij} + p_4 dt + p_{ijkl} d\epsilon_{ij} d\epsilon_{kl} + p_{ij4} d\epsilon_{ij} dt + p_4 dt^2 + p_{ijklmn} d\epsilon_{ij} d\epsilon_{kl} d\epsilon_{mn} + \dots \quad (1)$$

where:

$P =$ coefficient matrices, the subscripts refer to the components in the Cartesian coordinates x_i , $i = 1, 2, 3$, and number (4) refers to the time axis.

Since, dz must vanish as $d\epsilon_{ij} \rightarrow 0$ and $dt \rightarrow 0$, thus $P=0$. Setting $s=1$, and neglecting all quadratic terms, then $dz = P_4 \cdot dt$ which is of no interest, thus $P_4 = 0$. Setting $s=2$, and satisfying the conditions of isotropy, the quadratic form of Equation (1) can be written in terms of the first two invariants of $d\epsilon_{ij}$, as follows, (Bazant and Bhat,1976):

$$(dz)^2 = P_0 J_2 + (P_1 I_1 + P_2 dt)^2 + P_3 (dt)^2 \quad (2)$$

where:

$P_0, P_1, P_2, P_3 =$ non-negative coefficients.

$J_2 =$ second deviatoric strain increment invariant, and

$I_1 =$ first strain increment invariant.

Then, dz must vanish for both instantaneous time, $dt = 0$, and pure volumetric deformation, $J_2 = 0$, hence $P_1 = 0$. Thus, the remaining terms in Equation (2) can be rewritten in the following form:

$$(dz)^2 = \left(\frac{d\xi}{Z_1}\right)^2 + \left(\frac{dt}{\tau_1}\right)^2 \quad (3)$$

where:

$$d\xi = f_1(\sigma, \epsilon) \cdot d\zeta \quad (4.a)$$

$$d\zeta = \sqrt{J_2} = \sqrt{\frac{1}{2} de_{ij} \cdot de_{ij}} \quad (4.b)$$

$de_{ij} =$ deviatoric strain increment tensor

$$= d\epsilon_{ij} - \frac{1}{3} \delta_{ij} \cdot d\epsilon$$

$\delta_{ij} =$ Kronecker delta.

$d\epsilon =$ Volumetric strain increment $= d\epsilon_{kk}$

$z_I, \tau_I = \text{Constants.}$

$d\xi$ is scalar called “damage measure” that depends on strain increments and stresses to predict hardening and softening. $d\zeta$ is called “deformation measure” that depends on strain increments only. From Equations (3) and (4), $d\zeta$ and dz represent geometrically the length of path traced by material states in a six-dimensional strain space for $d\zeta$, or in a strain-time space for dz , (Ansal et al., 1979).

Secondly, generalizing of equations to three dimensions using dz instead of dt , and splitting the strain components into deviatoric and volumetric components to satisfy isotropy conditions, the following differential constitutive equations are deduced:

$$de_{ij} = \frac{dS_{ij}}{2G} + \frac{S_{ij}}{2G} \cdot dz \tag{5.a}$$

$$d\epsilon = \frac{d\sigma_m}{3k} + \frac{\sigma_m \cdot dt}{3k\tau_1} + d\lambda + d\epsilon^o \tag{5.b}$$

where:

$$de_{ij} = d\epsilon_{ij} - \frac{1}{3} \delta_{ij} \cdot d\epsilon$$

$$d\epsilon = d\epsilon_{11} + d\epsilon_{22} + d\epsilon_{33}$$

$d\lambda = \text{inelastic dilatancy,}$

$S_{ij} = \text{deviatoric stress tensor,}$

$$= \sigma_{ij} - \delta_{ij} \cdot \sigma_m$$

$$\sigma_m = \text{mean stress} = \frac{1}{3} \sigma_{kk}$$

$G, K = \text{shear and bulk elastic moduli, and}$

$d\epsilon^o = \text{stress-independent inelastic strains (e.g. thermal strains).}$

Both of the first terms of Equations (5.a) and (5.b) represent the elastic strain increments, while the remaining terms represent the inelastic strain increments. For instance, the term $(\sigma_m \cdot dt / 3K\tau_1)$ represents the time-dependent inelastic volumetric strain, i. e. creep, while $d\lambda$ represents the time-independent volumetric strain.

To develop a quasi-linear elastic incremental constitutive law for simplicity, the plastic stress increment tensor $d\sigma_{ij}^p$ can be obtained from Equations (5) by multiplying Equation (5.a) by $2G$, and Equation (5.b) by $3K$, hence:

$$\begin{aligned} d\sigma_{ij}^p &= 2G \cdot de_{ij}^p + \delta_{ij} (3K \cdot d\epsilon^p) \\ &= S_{ij} dz + \delta_{ij} (\sigma_m dt / \tau_1 + 3K d\lambda + 3K d\epsilon^o) \end{aligned} \tag{6}$$

The stress increments $d\sigma_{ij}$ are related to the elastic strain increments $d\epsilon_{ij}^e$ by the following equations:

$$d\sigma_{ij} = 2G \cdot de_{ij}^e + \delta_{ij} (3K \cdot d\epsilon^e) \tag{7}$$

Hence, the summation of Equations (7) and (8) yields:

$$d\sigma_{ij} + d\sigma_{ij}^p = D_{ijkl} \cdot d\epsilon_{kl} \tag{8}$$

where:

$$D_{ijkl} = \text{elastic coefficient matrix}$$

THE NUMERICAL PROCEDURE:

The basic constitutive law, Equation (5), is of a differential form, and the variables that govern inelastic deformations are (dz) and $(d\lambda)$. Bazant and Bhat (1976) used the step-by-step integration or step-iterative algorithm in which for each loading step, a number of iterations are performed till satisfaction of equilibrium of stresses and strains occurs. This is assured when the change in values of (dz) and $(d\lambda)$ for the same loading step becomes very small.

In this algorithm, the values of (dz) and $(d\lambda)$ computed from the previous loading step provide an initial estimate for the next loading step.

Endochronic Hardening Functions and Parameters:

The function f_1 in Equation (4) that accounts for hardening or softening, should decrease as the inelastic strains accumulate, because $d\xi$ is adopted as a measure of the accumulated inelastic strain, hence:

$$d\xi = \frac{d\eta}{f(\eta)} \quad ; \quad d\eta = F(\sigma, \epsilon) \cdot d\xi \quad (9)$$

where:

$f(\eta)$ = Strain-hardening function.

$F(\sigma, \epsilon)$ = Strain-softening function.

Thus, the function $f(\eta)$ has a significant effect on the non-linearity of the stress-strain relations, while the function $F(\sigma, \epsilon)$ allows for a gradual decrease of these relations on approach to peak stress. Both functions depend mainly on material type.

Hardening Functions and Dilatancy for Normally Consolidated Clays:

The function F in Equation (9) is determined semi-empirically from experimental data. The function F is governed by the effective confining stress I_1^σ , the volume change, I_1^ϵ , and the second deviatoric strain invariant, J_2^ϵ . Bazant et al. (1979) introduced the following formulation for function F :

$$F(\sigma, \epsilon) = a + \frac{|1 - a_1 I_1^\epsilon| / (1 + a_3 J_2^\epsilon)}{0.01 + a_2 (I_1^\sigma / Pa)} \quad (10)$$

where: a 's = material constants.

Pa = atmospheric pressure = 101.3 kN/m²

The division of I_1^σ in Equation (10) by Pa is to make the relation dimensionless. Constant "a" must be positive to ensure irreversible strain increment for the critical case of no hardening or softening, (Bazant et al., 1979).

The function $f(\eta)$ represents the limiting critical case of no hardening or softening. Thus, for large values of η , this function, $f(\eta)$, must converge to one. The function $f(\eta)$ takes the following form:

$$f(\eta) = 1 + \frac{\beta_1}{1 + \beta_2 \eta} \quad (11)$$

where: β_1 and β_2 = constants.

The dilatancy or densification function $d\lambda$ of clays depends on shear and volumetric stresses and strains. Hence, the function $d\lambda$ depends on J_2^ϵ , I_1^σ and I_1^ϵ . Moreover, $d\lambda$ depends on λ itself because the volumetric strain increment should decrease monotonically till zero as a limit in the case of failure. Hence $d\lambda$ is equal to (Bazant et al., 1979):

$$d\lambda = \frac{C_o |1 + C_1 I_1| d\zeta}{(1 + C_2 I_1^\sigma / Pa)(1 + C_3 J_2^\epsilon)(1 + C_4 \lambda)} \tag{12}$$

where: c_o, c_1, c_2, c_3, c_4 = material constants.

$d\lambda$ is determined empirically from tests and it depends on the clay type, stress path and stress history.

The tensile strengths of soils are very small and hence neglected.

The elastic moduli G and K of the soil element change during loading, and thus the accumulated densification-dilatancy measure λ and the effective normal stress also change. Thus, the effect of void ratio is:

$$\frac{de}{e_o} = \frac{\epsilon_v (1 + e_o)}{e_o} = \frac{3(1 + e_o) \lambda}{e_o} = \frac{3\lambda}{n} \tag{13}$$

where: e_o = initial void ratio

ϵ_v = volumetric strain = ϵ_{kk}

n = porosity.

while the effect of normal stress is the ratio $(I_1^\sigma - I_1^{\sigma_o}) / I_1^{\sigma_o}$, where $I_1^{\sigma_o}$ is the initial first stress invariant. Hence, the elastic moduli will be equal to:

$$G = G_o \left(1 + b_1 \frac{I_1^\sigma - I_1^{\sigma_o}}{I_1^{\sigma_o}} + b_2 \frac{3\lambda}{n} \right) \tag{14}$$

where: b_1 and b_2 = constants,

$$\text{and } K = \frac{2}{3} G(1 + \nu) / (1 - 2\nu) \tag{15}$$

Model Parameters of Clays:

All material parameters in the previous equations are based on best fit of experimental results.

Constant “a” in Equation (10) affects the value of the peak stress. Constant a_3 which is called “distortion coefficient” is determined by the following correlation proposed by Ansal et al. (1979). Based on general pattern of results:

$$a_3 = 153.8(e_o Pa / P_o) + 34.62 \tag{16}$$

where:

P_o = consolidation pressure.

Similarly, the plasticity coefficient Z_1 in Equation (3) that accounts for rigidity and deformability of clays, is determined from the following correlation:

$$Z_1 = 0.00294(e_o P_o / P_a)^2 - 0.0177(e_o P_o / P_a) + 0.0396 \tag{17}$$

Ansal et al. (1979) determined an approximate correlation for densification coefficient C_o in Equation (12), softening coefficient β_2 in Equation (11), and the elastic modulus E , as shown in Figure (1). This correlation depends on the consolidation pressure P_o , and the liquidity index of the clay I_L , where (Mitchel, 1993):

$$I_L = \frac{w_{nat} - w_p}{I_p} \tag{18}$$

where:

w_{ant} = natural water content.
 w_p = plastic limit
 I_p = plasticity index = $w_L - w_p$
 w_L = liquid limit.

Choice of appropriate ratio of the liquidity index to the consolidation stress is tempered by judgement in the absence of test results.

All other constants are determined experimentally. The values of the parameters as proposed by Bazant et al. (1979) are shown in Table (1):

Table (1) – Material parameters of endochronic model for normally consolidated clays.

Parameter	Value
a_0	4
a_1	500
a_2	0.75
β_1	5n (n = porosity)
C_1	2500
C_2	0.25
C_3	1000
C_4	9000
b_1	0.1
b_2	0.1

Computer Program:

The computer program **Endoch**, coded in Fortran language, was written by the authors. The algorithm used in the endochronic model incorporates an iterative procedure. The program computes stresses, strains, all functions like F , $f(\eta)$, and variables like λ , η , at mid-step loading. Iterations are then performed till the tolerance of the values of dz and $d\lambda$ becomes less than 0.05 %. The values of strain increments, $d\varepsilon$, intrinsic time, dz , and inelastic dilatancy, $d\lambda$, or the previous step are taken as an estimate for the current step.

APPLICATIONS:

This model have been applied for simulating stress-strain relationships of two Iraqi soils:

i) First application

Al- Mufty (1990) carried out a series of tests on al-Fao soft clay. Block samples were obtained from an area close to the river Shatt-Al-Arab.

The top layer of Fao soil was found to be stiff to very stiff brownish gray silty clay with a desiccated crust. This layer is followed by a soft to very soft gray silty clay.

According to the unified classification system, the soil from both layers may be classified as CL-CH, inorganic clays of medium to high plasticity. According to, AASHTO M145-73, the soil is classified as A-7-6 (16).

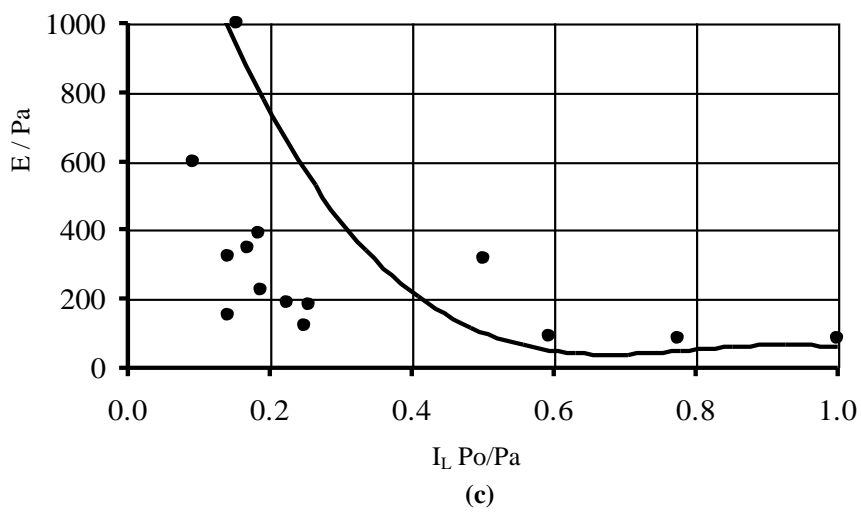
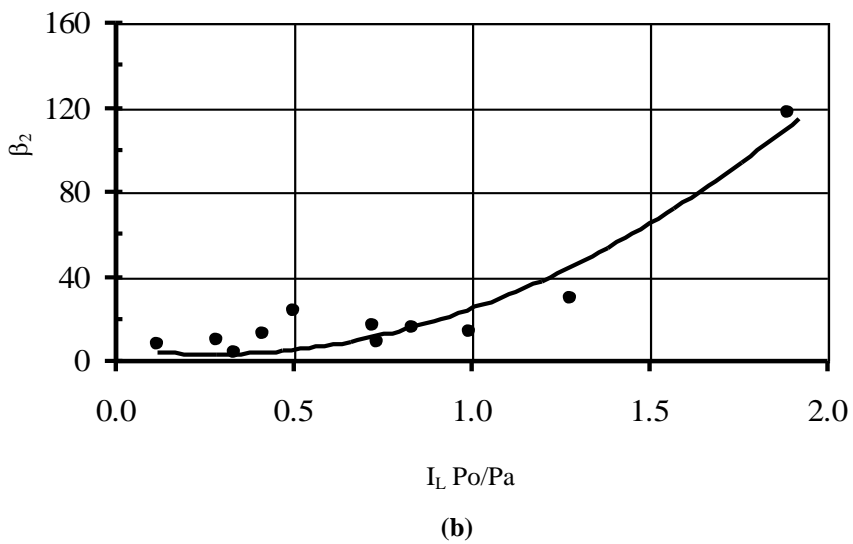
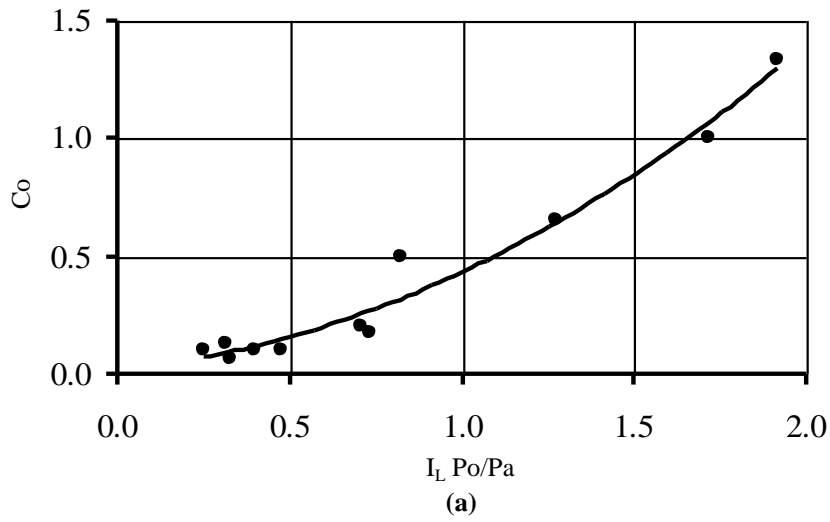


Fig. (1) – Approximate correlation for:
a) Densification coefficient, C_o .
b) Softening coefficient, β_2 .
c) Elastic modulus, E .

The average properties of the soil at sampling depths 1.25 m and 3 m respectively are listed in Table (2).

Table (2) - Average properties of the soft clay from Al-Fao, (from Al-Mufti, 1990).

Property	1.25 m depth	3 m depth
Total unit weight γ_t , kN/m ³	17.9	17.7
Water content w %	30	45
Liquid limit w_L %	54	50
plasticity index I_p %	27	24
Liquidity index I_L	0.11	0.79
Specific gravity G	2.7	2.72
Sand size fraction %	9	12
Silt size fraction %	58	60
Clay size fraction %	33	28
Activity A	0.82	0.86

Among the tests carried out by Al-Mufti (1990) unconsolidated undrained triaxial compression tests on samples compacted by the standard compaction test to the maximum dry density and optimum moisture content. These results are compared with those predicted by the endochronic model in Figures (2) to Figure (6).

Figures (2) and (3) represent the samples that are taken from the top layer, and the figures from (4) to (6) represent the samples that are taken from the layer below the top layer.

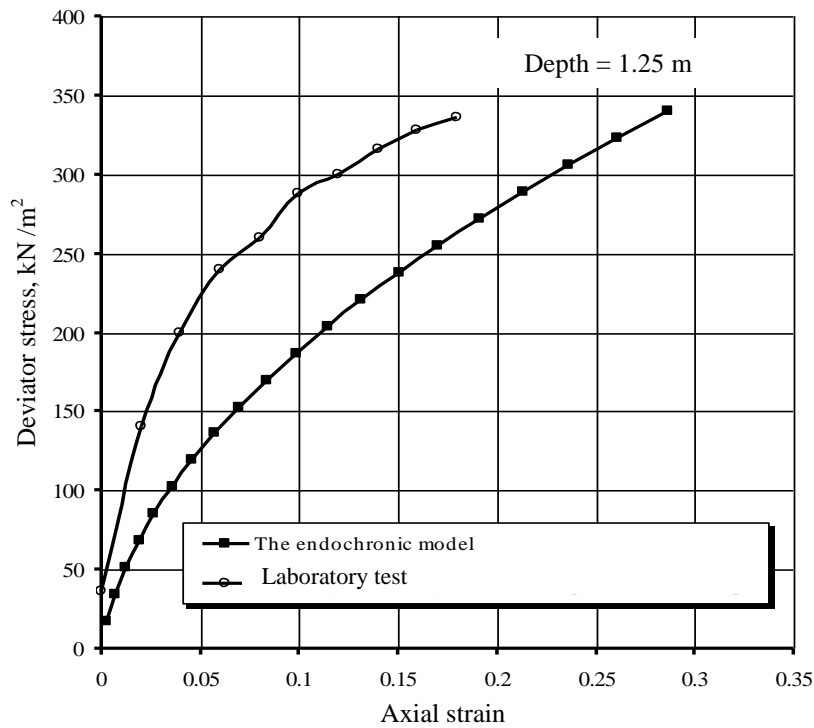


Fig. (2) - A comparison between the stress-strain relationships predicted by the endochronic model with laboratory tests of Al – Mufty (1990), $\sigma_3 = 300$ kPa.

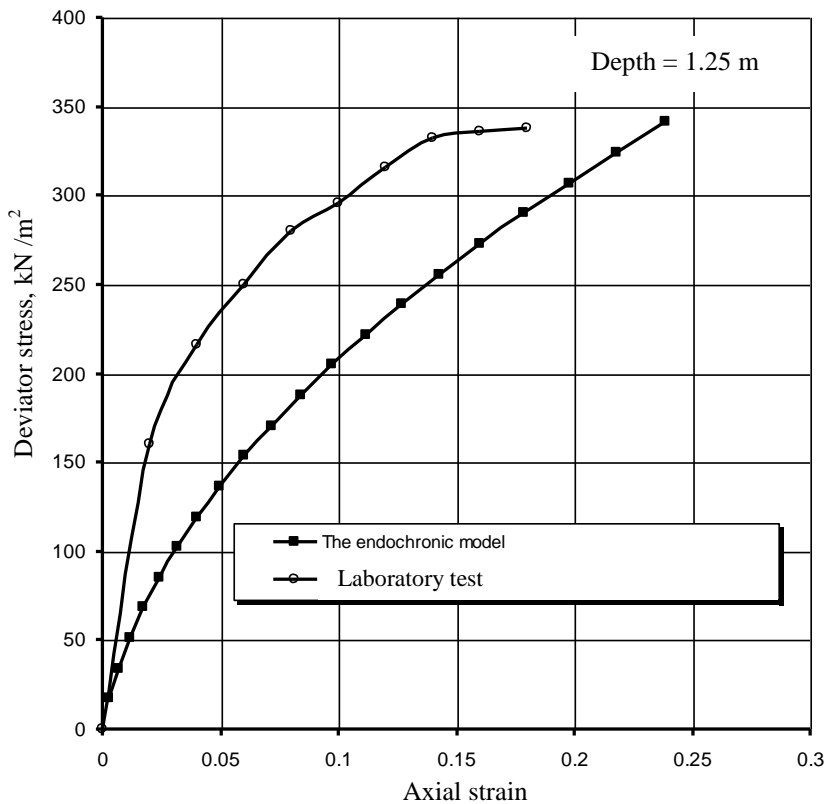


Fig. (3) - A comparison between the stress-strain relationships predicted by the endochronic model with laboratory tests of Al – Mufty (1990), $\sigma_3 = 300$ kPa.

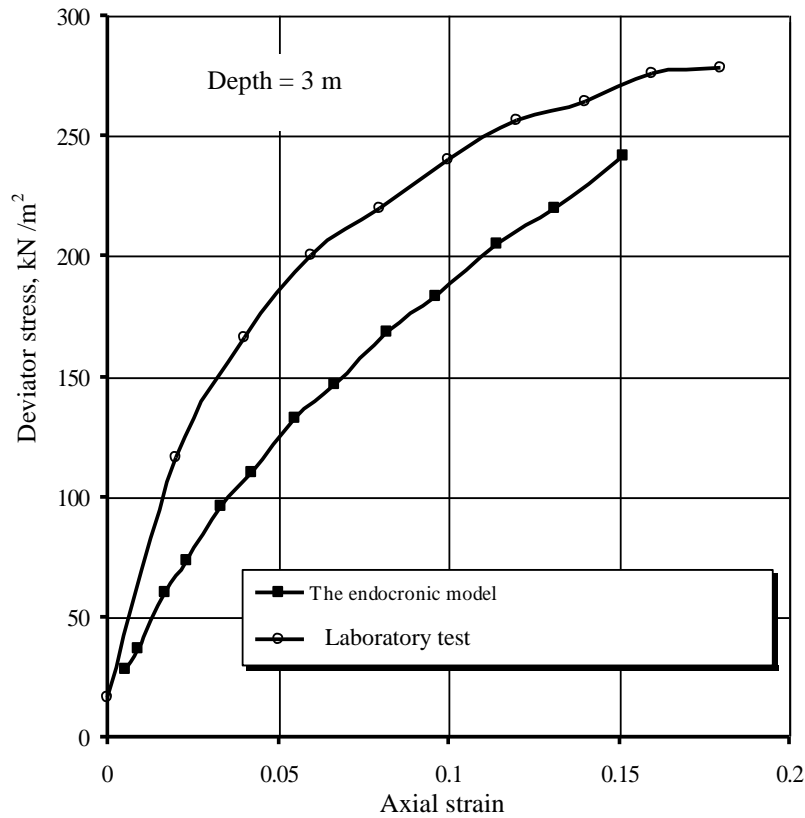


Fig. (4) - A comparison between the stress-strain relationships predicted by the endochronic model with laboratory tests of Al – Mufty (1990), $\sigma_3 = 100$ kPa.

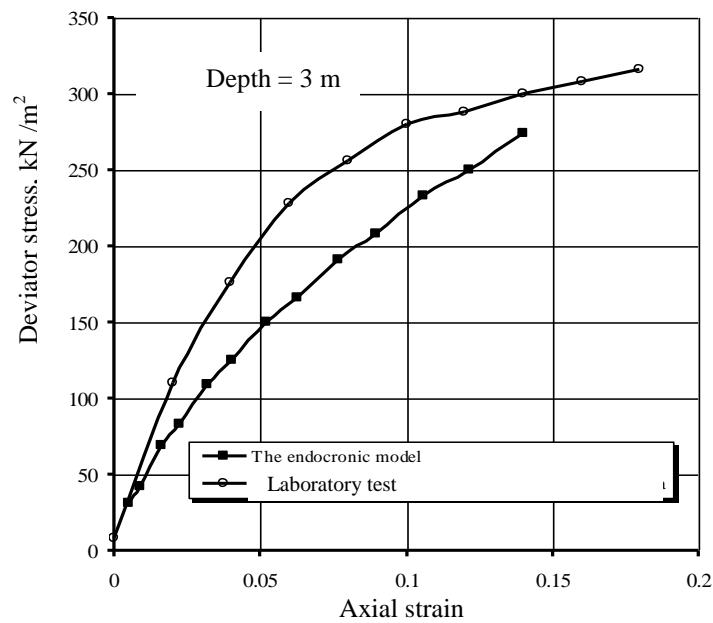


Fig. (5) - A comparison between the stress-strain relationships predicted by the endochronic model with laboratory tests of Al – Mufty (1990), $\sigma_3 = 200$ kPa.

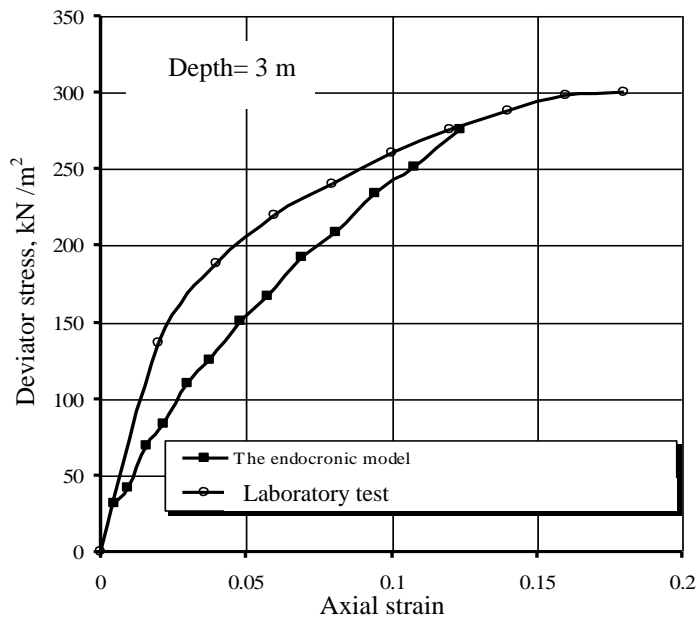


Fig. (6)- A comparison between the stress-strain relationships predicted by the endochronic model

with laboratory tests of Al – Mufty (1990), $\sigma_3 = 300$ kPa.

It can be observed in these figures that the model overestimates the strains for all the cases studied under high stress increments.

In addition, there is no definite yield point can be obtained. Thus it is approximately suitable for normally consolidated clays where ductile behaviour of the stress-strain is expected.

ii) Second application

Al- Saady (1989) carried out laboratory tests on an A-6 soil during construction of a road embankment. A representative area located at Al – Zafarania (south of Baghdad), was chosen for the research. The site covers an area of soil composed of silty clay with varying thickness. This stratum behaves as normally or slightly overconsolidated soil, have an upper desiccated crust 0.5-0.75 m thick.

The distribution of the particle sizes indicated:

Clay fraction = 45 %, silt fraction = 37 %, sand fraction = 18 %.

It is classed as “CL” in a Casagrande classification chart.

Among the tests carried out by Al- Saady (1989) consolidated undrained triaxial test which was designated as series D as shown in Table (3).

In addition, unconsolidated undrained triaxial test which was designatd as series G as shown in Table (4).

Consolidated undrained triaxial test results are compared with those predicted by the endochronic model in Figures (7) to (12) which show a comparison between the stress-strain relationships predicted by the endochronic model with laboratory tests of Al – Saady, (series, D).

Consolidated drained triaxial test results are compared with those predicted by the endochronic model in Figures (13) to (18). Figures (19) to (24) show a comparison between the volumetric strain–axial strain relationships predicted by the endochronic model with laboratory tests of Al-Saady, (series, G).

Table(3) - The results of series (D), (from Al-Saady, 1989).

Test No.	σ'_c kN/m ²	e_o	w_c %	$(\sigma_1 - \sigma_3)_f$ kN/m ²	$(\sigma_1 / \sigma_3)_f$ kN/m ²	Δu_f kN/m ²
1	79	0.76	26.0	123.24	3.50	30.81
2	100	0.70	24.3	123.00	3.55	52.22
3	150	0.74	25.6	189.21	3.30	72.45
4	200	0.69	24.6	219.60	3.25	104.45
5	300	0.75	25.4	279.00	3.25	176.68
6	376	0.73	26.0	348.01	3.30	224.07

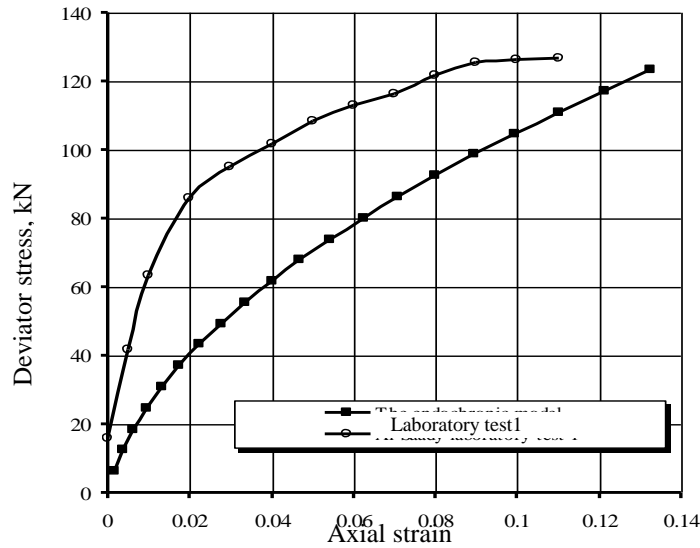


Fig. (7) - A comparison between the stress-strain relationship predicted by the endochronic model with laboratory tests of Al – Saady, Test 1, Series D.

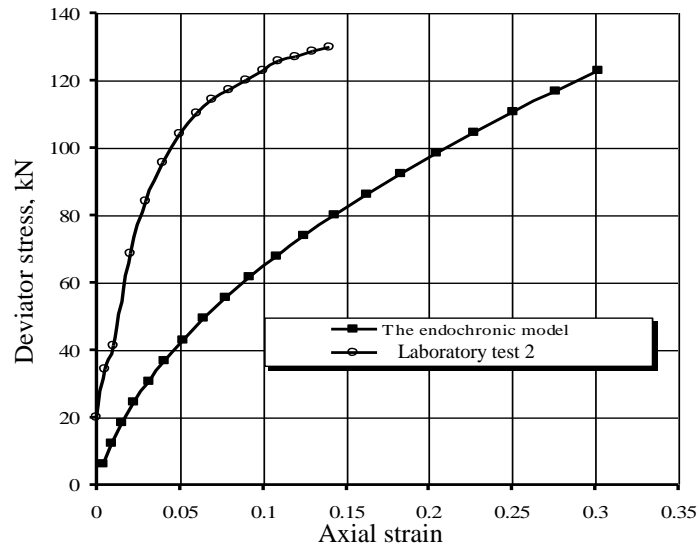


Fig. (8) - A comparison between the stress-strain relationship predicted by the endochronic model with laboratory tests of Al – Saady, Test 2, Series D.

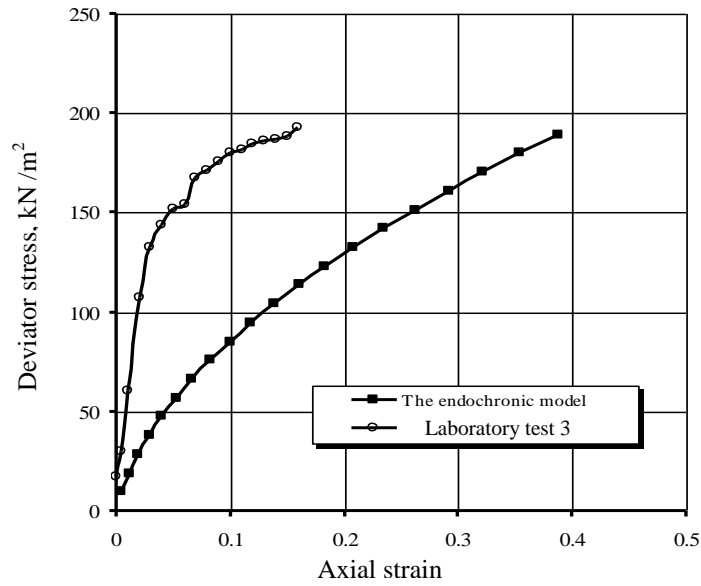


Fig. (9) - A comparison between the stress-strain relationship predicted by the endochronic model with laboratory tests of Al – Saady, Test 3, Series D.

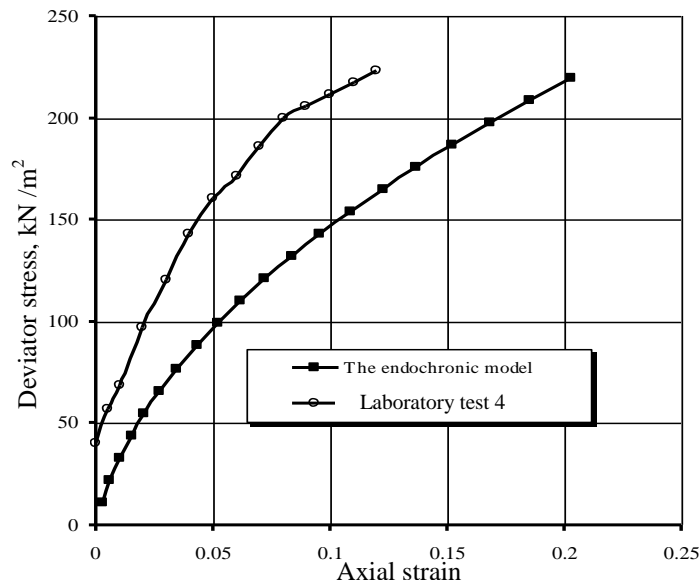


Fig. (10) - A comparison between the stress-strain relationship predicted by the endochronic model with laboratory tests of Al – Saady, Test 4, Series D.

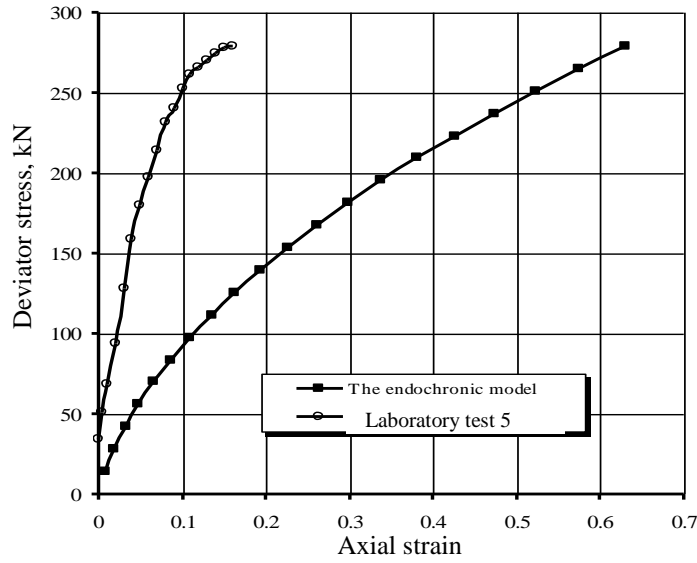


Fig. (11) - A comparison between the stress-strain relationship predicted by the endochronic model with laboratory tests of Al – Saady, Test 5, Series D.

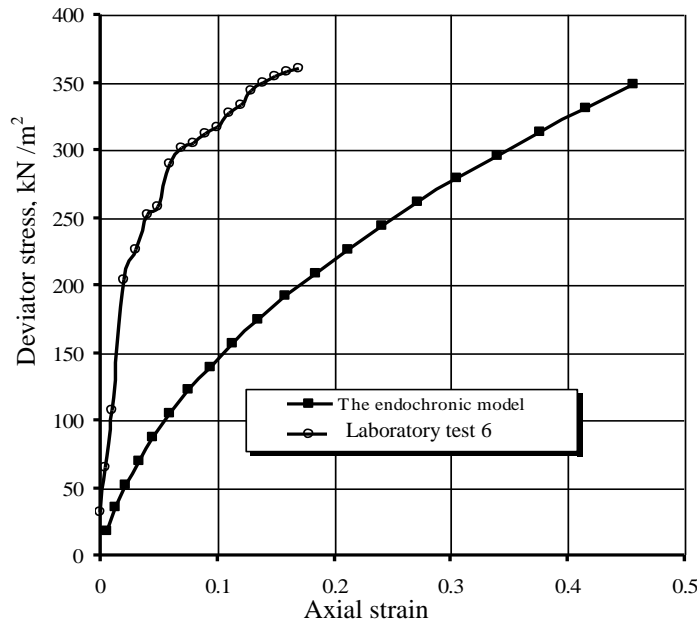


Fig. (12) - A comparison between the stress-strain relationship predicted by the endochronic model with laboratory tests of Al – Saady, Test 6, Series D.

Table (4) - The results of series (G), (from Al-Saady, 1989).

Test No.	σ'_c kN/m ²	e_o	w_c %	$(\sigma_1 - \sigma_3)_f$ kN/m ²	$\left(\frac{\Delta V}{V_o}\right)_f$ kN/m ²
1	79	0.66	23.5	198.87	2.300
2	100	0.69	24.7	281.18	2.283
3	150	0.75	26.0	348.03	3.026
4	200	0.75	27.0	405.03	3.016
5	300	0.69	25.2	752.55	3.590
6	376	0.72	25.0	913.52	3.710

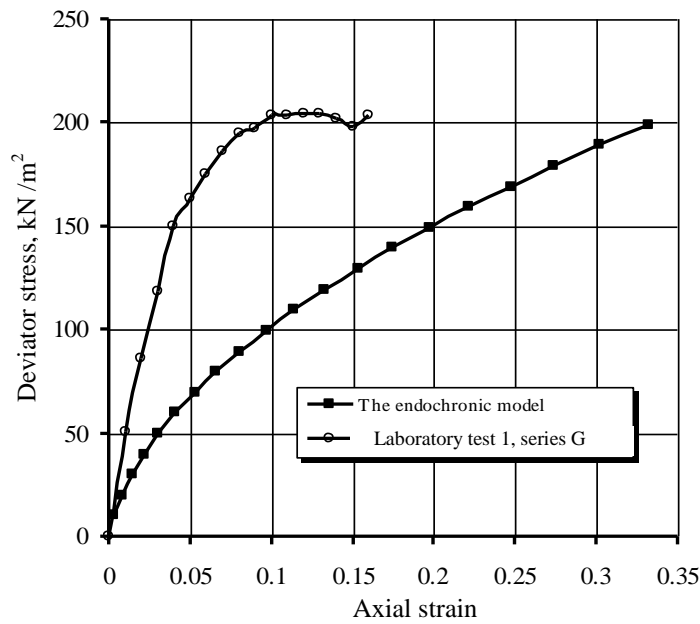


Fig. (13) - A comparison between the stress-strain relationship predicted by the endochronic model with laboratory tests of Al – Saady, Test1, series G.

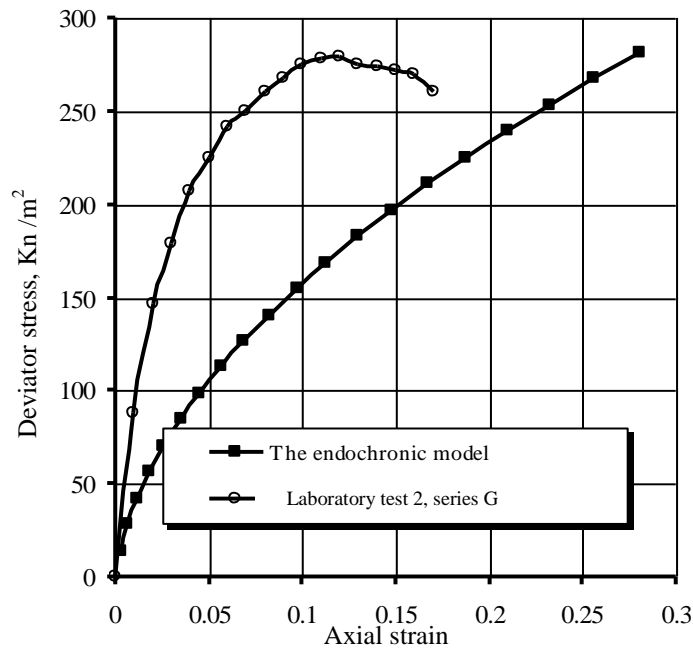


Fig. (14) - A comparison between the stress-strain relationship predicted by the endochronic model with laboratory tests of Al – Saady, Test2, series G.

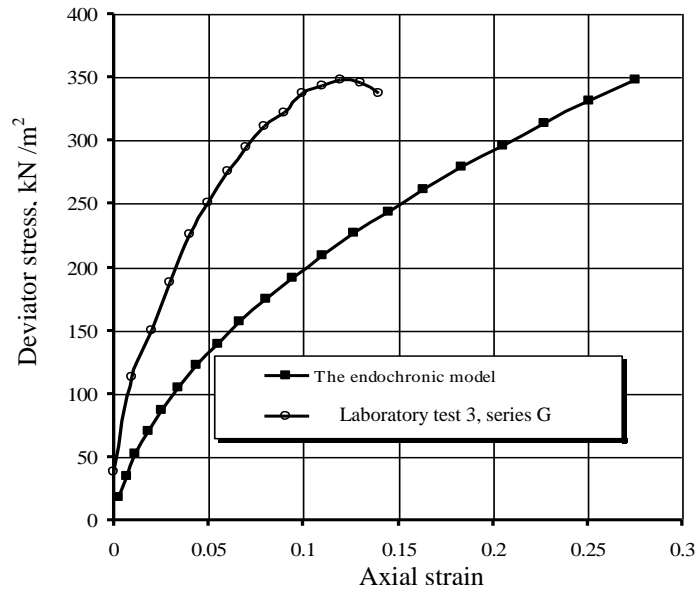


Fig. (15) - A comparison between the stress-strain relationship predicted by the endochronic model with laboratory tests of Al – Saady, Test3, series G.

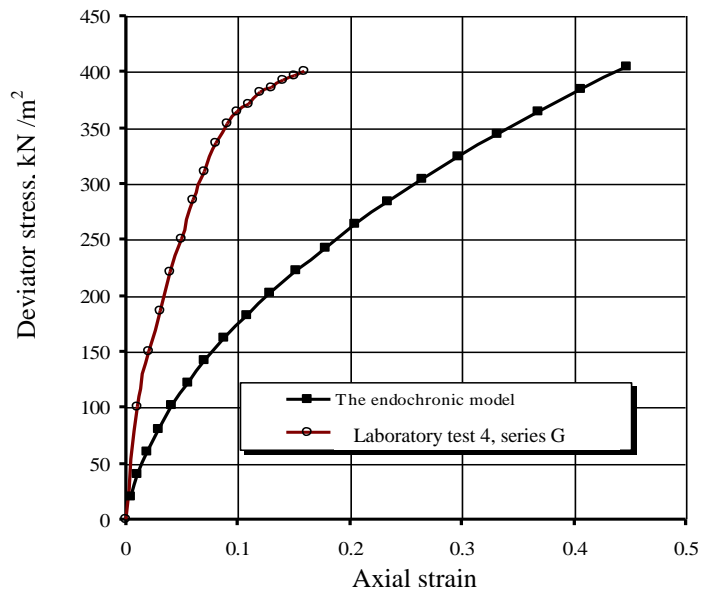


Fig. (16) - A comparison between the stress-strain relationship predicted by the endochronic model with laboratory tests of Al – Saady, Test4, series G.

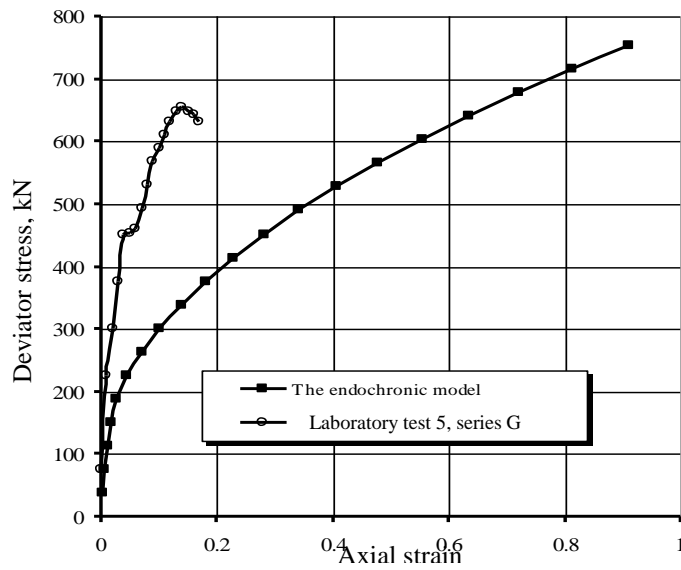


Fig. (17) - A comparison between the stress-strain relationship predicted by the endochronic model with laboratory tests of Al – Saady, Test5, series G.

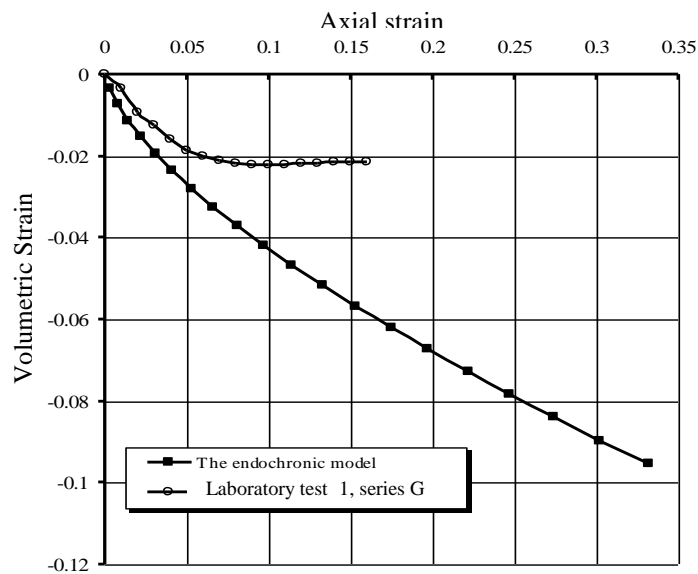


Fig. (18) - A comparison between the volumetric strain – axial strain relationship predicted by the endochronic model with laboratory tests of Al – Saady, Test1, series G.

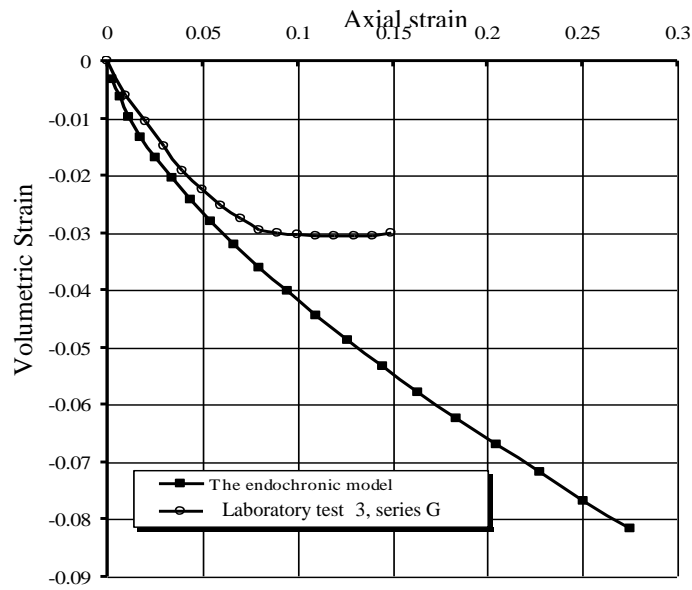


Fig. (19) - A comparison between the volumetric strain – axial strain relationship predicted by the endochronic model with laboratory tests of Al – Saady, Test2, series G.

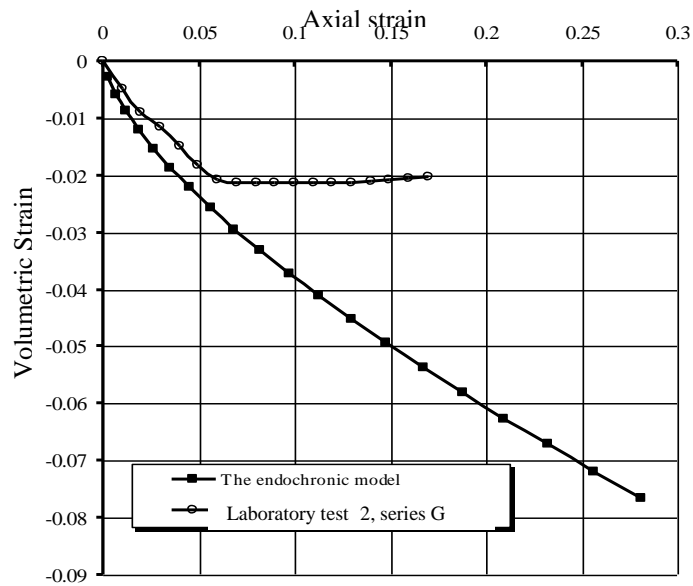


Fig. (20) - A comparison between the volumetric strain – axial strain relationship predicted by the endochronic model with laboratory tests of Al – Saady, Test3, series G.

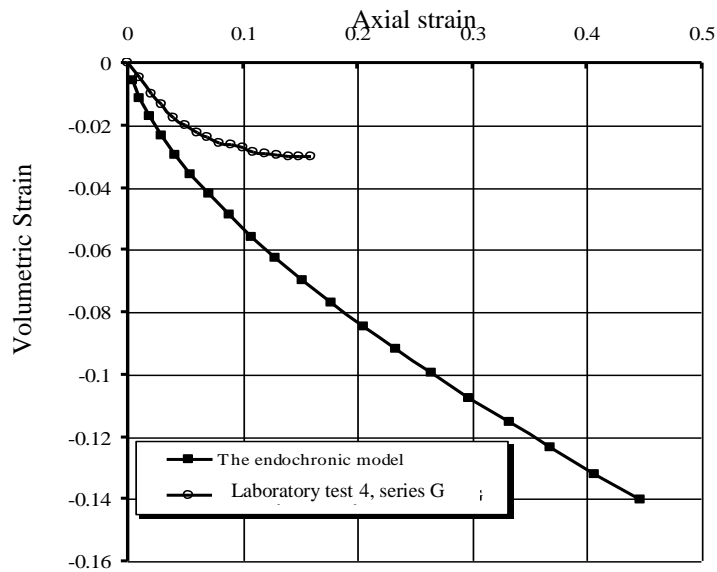


Fig. (21) - comparisons between the volumetric strain – axial strain relationship predicted by the endochronic model with laboratory tests of Al – Saady, Test 4, series G.

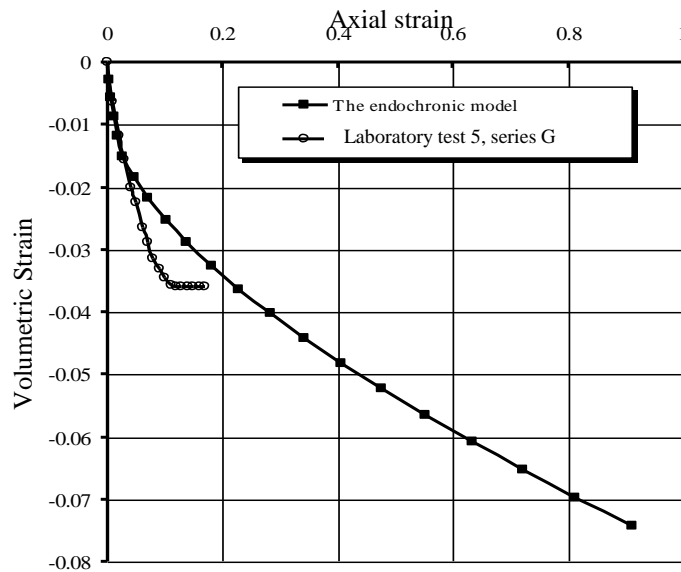


Fig. (22) - A comparison between the volumetric strain – axial strain relationship predicted by the endochronic model with laboratory tests of Al – Saady, Test 5, series G.

The same behaviour is noticed in this clay. The predicted volumetric strains are closer to measured strains under small stress increments. At large stresses, the predicted strains became larger.

CONCLUSIONS:

- The endochronic model overestimates the strains for all the cases simulated under high stress increments.
- There is no definite yield point can be obtained when simulating the laboratory tests. This means that this model can be adopted for normally consolidated clays where ductile behaviour of the stress-strain is expected.
- The error in simulation may be attributed to the model parameters, which need to be evaluated by carrying out parametric study for Iraqi clays.

REFERENCES:

- Al-Muftay, A. A. E., (1990). (Analysis of Stress Deformation Behaviour of Fao Soil), M.Sc. thesis, Civil Engineering Department, University of Baghdad.
- Al- Saady, N. H., (1989). (Analysis of an A-6 Soil During Construction of Road Embankment), M.Sc. thesis, Civil Engineering Department, University of Baghdad.
- Ansal, A. M., Bazant, Z. P. and Krizek, R. J., (1979). (Viscoplasticity of Normally Consolidated Clays), Journal of Geotechnical Engineering, ASCE, Vol. 105, No. GT4, p.p. 519 – 537.
- Bazant, Z. P. and Bhat, P. D. (1976). (Endochronic Theory of Inelasticity and Failure of Concrete), Journal of Engineering Mechanics, ASCE, Vol. 102, No. EM4, p.p. 701 – 722.
- Bazant, Z. P., Ansal, M. and Krizek, R. J., (1979). (Visco-Plasticity of Transversely-Isotropic Clays), Journal of Engineering Mechanics, ASCE, Vol. 105, No. EM5, p.p. 549 – 565.
- Mitchel, J. K. (1993). (Fundamentals of Soil Behaviour), Second Edition, John Wiley and Sons.
- Valanis, K. C., (1971). (A Theory of Viscoplasticity without a Yield Surface – Part I: General Theory, Part II: Application to Mechanical Behaviour of Metals), Archives of Mechanics, Vol. 23, No. 4, p.p. 517 – 551, Warszawa.

NOTATION:

$d \in_{ij}$	Strain increments
dt	Time increments
P	Coefficient matrices
J_2	second deviatoric strain increment invariant
I_1	first strain increment invariant
de_{ij}	deviatoric strain increment tensor
δ_{ij}	Kronecker delta
$d \in$	Volumetric strain increment
z_1, τ_1	Constants
$d\xi$	damage measure
$d\zeta$	deformation measure
$d\lambda$	inelastic dilatancy
S_{ij}	deviatoric stress tensor
σ_m	mean stress
G	shear elastic moduli
K	bulk elastic moduli
$d \in^o$	stress-independent inelastic strains
$d\sigma_{ij}$	The stress increments
D_{ijkl}	elastic coefficient matrix



$d \in_{ij}^e$	elastic strain increments
$f(\eta)$	Strain-hardening function.
$F(\sigma, \epsilon)$	Strain-softening function.
I_1^σ	effective confining stress
I_1^ϵ	the volume change
J_2^ϵ	the second deviatoric strain invariant
a's	material constants
Pa	atmospheric pressure
β_1	constants
c's	material constants
β_2	softening coefficient
e_o	initial void ratio
ϵ_v	volumetric strain
n	porosity
b's	constants
Po	consolidation pressure
C_o	densification coefficient
E	elastic modulus
I_L	the liquidity index of the clay
w_{ant}	natural water content.
w_p	plastic limit
I_p	plasticity index
w_L	liquid limit.